MOLECULAR DYNAMICS SIMULATIONS OF AQUEOUS SOLUTIONS OF IONIC LIQUIDS

Karel MATAS[1,*] and Jiří KOLAFA[2]

Department of Physical Chemistry, Institute of Chemical Technology, Prague, 166 28 Prague 6, Czech Republic; e-mail: [1] karel.matas@vscht.cz, [2] jiri.kolafa@vscht.cz

Received October 6, 2009
Accepted November 13, 2009
Published online March 15, 2010

Dedicated to Professor Ivo Nezbeda on the occasion of his 65th birthday.

We performed a molecular dynamics study of aqueous solutions of ionic liquids 1-butyl-3-methylimidazolium chloride ([BMIM]Cl) and 1-octyl-3-methylimidazolium chloride ([OMIM]Cl) in order to elucidate the anomalous dependence of the surface tension on concentration. We found that cations are placed preferably at the surface with alkyl chains pointing towards vacuum. Anions compensate the surplus of a positive charge on the surface by forming a layer below the cation layer. At lower concentrations the surface tension decreases with concentration. At higher concentrations the surface becomes saturated by cations and the decrease slows down. The decrease of surface tension with concentration is a consequence of the structural changes, although the experimentally observed anomalous increase at even higher concentrations was not reproduced.
Keywords: Molecular dynamics; Ionic liquid; Interfaces; Imidazolium salts; Surface tension.

Ionic liquids (ILs)[1,2] and room temperature ionic liquids (RTILs) are organic salts with melting points below 100 and 25 °C, respectively. In recent years they have rapidly developed as new solvents for synthesis and catalysis. For their vanishingly small vapour pressure[3,4] as well as low toxicity (of at least some RTILs) they are often called "green solvents".

Thanks to a wide spectrum of possible cation–anion combinations it is nearly impossible to explore even a small fraction of possible RTILs. However, the same variability enables to design RTILs fitted to a particular application (e.g., hydrophobic or hydrophilic RTIL, RTIL with desired miscibility, ...). RTILs are often noted as "designer solvents". The newest generation of RTILs is called "task-specific ionic liquids", which refers to the growing interest in cations with chains modified for a specific use (e.g., polar, chiral or fluorinated).

Collect. Czech. Chem. Commun. 2010, Vol. 75, No. 3, pp. 333–348

doi:10.1135/cccc2009518

Understanding RTILs at the molecular level is a key to mastering their design. RTILs are different from "normal" molecular liquids. Some of the well-known rules, assumptions and also experimental methods about liquids cannot be easily transferred to RTILs. However, many physicochemical properties are known and are available in public databases.

Most experiments deal with bulk properties of ionic liquids. Less frequent studies of surfaces of ionic liquids include sum-frequency generation spectroscopy (SFG)[5–7], neutron and X-ray reflextion[8], surface tension[9], direct recoil spectroscopy[10–12] and photoelectron spectroscopy[13]. A special attention is paid to surface orientation of ions. Santos and coworkers[5] performed a SFG and X-ray crystallography study of orientation and interfacial location of the pure 1-butyl-3-methylimidazolium ($[BMIM]^+$; Fig. 1) methylsulfate and 1-butyl-3-methylimidazolium methanosulfonate. They claimed that both the cation and anion occupy the first layer at the gas–liquid interface with methyl and butyl groups of the cation directed to the gas phase. The effect of temperature and anion on the orientation of the cation is small[14].

In contrast to the pure RTIL/air interface, the RTIL–water/air interface is strongly influenced by the nature of RTIL ions. Hydrophobic RTILs contain for instance $[PF_6]^-$ or $[AsF_6]^-$ ions, hydrophilic ones may contain $[BF_4]^-$. Water molecules interact preferentially with anions[15] and the interface becomes highly structured. Water affects the surface of hydrophilic RTILs more than hydrophobic. The aromatic circle of hydrophilic RTILs is oriented preferentially along the surface, but the aromatic circle of the hydrophobic ones is oriented along the surface normal.

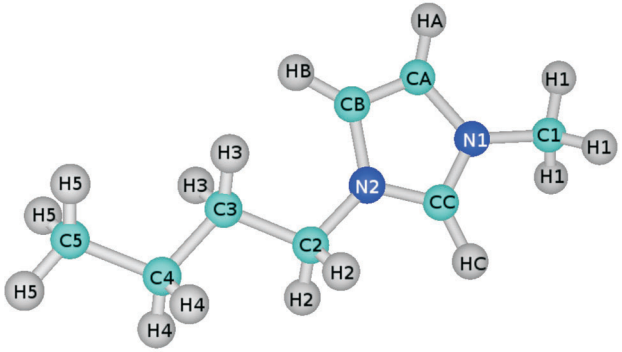

FIG. 1
Atom numbering in the $[BMIM]^+$ cation

Bowers et al.[9] and Sung et al.[7] studied the surface tension of aqueous solutions of [BMIM][BF_4] and [BMIM][PF_6]. The surface tension decreases until it reaches a plateau or starts a slow increase (which is barely discernible). The critical molar fraction at which this effect occurs for [BMIM][BF_4] is about 0.015 (Bowers), for [BMIM][PF_6] 0.016 (Sung). From SFG they concluded that at low concentrations the surface is populated only with cations. Anions start to appear at higher concentrations, compensating the charge of cations. Due to the increase of electrostatic interactions this may cause the surface tension to increase.

Picálek et al.[16] performed a set of molecular dynamics simulations in order to understand this phenomenon at molecular level and judge a difference between polarizable and non-polarizable force fields. The structure of the interface was reproduced, but the increase of the surface tension was observed for a polarizable force field only and barely above the statistical error.

In this work, we extend this study to more hydrophobic and surface active RTILs with longer chains.

SIMULATIONS

All simulations were performed with the molecular modeling and simulation package MACSIMUS [17] in the NVT ensemble and slab geometry[18].

The used force fields were Liu[19] for ILs and TIP4P/2005 for water[20]. The partial charges of the models are listed in Table I; for the TIP4P/2005 model see ref.[20]. Missing atomic charges of 1-octyl-3-methylimidazolium ($[OMIM]^+$) were obtained from quantum chemical calculations with Gaussian 03W [21] program (CHELPG method and basis set B3LYP/6-31++g**). The cross Lennard–Jones interactions are given by the Lorentz–Berthelot combining rules.

A slab is a 2D layer perpendicular to the *z*-axis of the simulation box, which is periodic in the *x*- and *y*-directions. Hence the *z*-side of the simulation box should be several times longer than the *x*- and *y*-sides. We used a box of size 30 × 30 × 75 Å. The number of molecules was chosen so that the slab widths of aqueous systems were about 30 Å. This is given by formula $n_w = 1000 - 10 \times n_i$, where n_w is the number of water molecules and n_i the number of ion pairs.

The simulation temperature was set to 300 and 360 K. The Berendsen thermostat[22] with correlation time of 1 ps was used. The equations of motion were integrated using the Verlet's algorithm[23] with a timestep of 1 ps. The bond lengths were constrained by the SHAKE algorithm[18].

Long-range Coulombic interactions were accounted for by the 3D Ewald summation method[18] with the correction to slab dipole[24]. This correction adds to the interaction potential a homogeneous electric field (in the *z*-direction) which exactly cancels the field of the periodic assembly of layers repeating in the *z*-direction. The system is thus equivalent to an *x*,*y*-periodic slab because the higher-order (quadrupolar) terms in the *z*-direction are much weaker. The boudary condition is no longer periodic in the *z*-direction, however, no particles are allowed to cross the basic cell *z*-boundary.

The Lennard–Jones cutoff was set to 13 Å. Corrections to the surface tension were calculated using the *z*-density profiles[16].

The surface tension γ was calculated by the formula

$$\gamma = -(3/4)\, L_z\, (p - p^s) \qquad (1)$$

where L_z is the length of the simulation box, p the virial pressure (as calculated from the simulation) and p^s the vapor pressure. Formula (*1*) is based on the standard formula with the normal and tangential components of

TABLE I
Partial atomic charges (in e). Atoms C5–C8 in OMIM correspond to groups CH_2 in the chain, C9 to the terminating CH_3 (for atom numbering see Fig. 1)

Atom	BMIM	OMIM	Atom	BMIM	OMIM
CA	–0.1426	–0.0963	HA	0.2340	0.1929
CB	–0.2183	–0.1648	HB	0.2633	0.2209
CC	–0.0055	–0.0780	HC	0.2258	0.2159
C1	–0.0846	–0.1676	H1	0.1085	0.1266
C2	–0.0153	–0.1113	H2	0.0796	0.0856
C3	0.0107	0.1643	H3	0.0204	–0.0308
C4	0.0309	0.0426	H4	0.0157	–0.0059
C5	–0.0713	0.0215	H5	0.0294	–0.0079
C6	–	0.0267	H6	–	–0.0128
C7	–	0.0162	H7	–	–0.0104
C8	–	0.0179	H8	–	–0.0404
C9	–	–0.1531	H9	–	0.0334
N1	0.0596	0.1164	N2	0.0682	0.1403
Cl	–1.0000				

pressure. However, the normal components in the slab geometry are proportional to the saturated vapor pressure which is essentially zero. The advantage of formula (*1*) is that in the Ewald summation one can, instead of calculating all (*r*- and *k*-space) components of the pressure tensor, make use of the virial theorem (the isotropic virial equals minus the electrostatic energy). During development of the code, we tested also the virtual volume change (to get the isotropic presure) and virtual area methods. (On the other hand, we must admit, based on our recent calculations, that the results of (*1*) are more noisy and probably it is more efficient to calculate the full pressure tensor.)

The simulations were started from a lattice configuration at very low density so that no overlap may occur. The box was then gradually scaled down until the desired size was achieved. The slab with a symmetric distribution of ions was created using additional forces which repelled molecules from the space below and above the slab. The system was intensively cooled during this process (the thermostat correlation time was set to 0.1 ps). After achieving a stable slab, the additional forces were removed and only small forces restraining molecules from moving periodically in the *z*-direction (at both ends of the simulation box) were kept on.

The systems were equilibrated for about 0.5–1 ns. The production runs of aqueous systems lasted 4–8 ns.

RESULTS AND DISCUSSION

All concentrations are presented as total mole fraction of the ionic liquid. The bulk concentration cannot be determined accurately enough (It is possible, e.g., from the density profiles. But due to a small number of RTIL molecules, the value of the bulk mole fraction exhibits large fluctuations.) and therefore is presented only for comparison.

Structure of the Surface and Ion Dynamics

From the density profiles (The histogram of the distribution of selected atoms across the slab. Similarly the charge profiles are histograms of the distribution of charges across the slab. The presented density profiles are normalized to the same integral, i.e., areas under under the curves are the same.) (Figs 2 and 3) it is apparent that the distributions are asymmetric (especially at lower temperatures and for lower concentrations). This effect is caused by slow dynamics. Not only the ions once adsorbed at the surface

dissolve only slowly into the bulk, but also the diffusion across the slab is slow in the timescale of nanoseconds.

Cations prefer the surface. Their positive charge is at lower concentrations compensated mostly by asymmetric solvation, at higher concentrations by anions which begin to form a layer close to the surface, but only rarely right in the topmost cation-rich layer. The asymmetric solvation (see the anion density profiles in Figs 2 and 3) means that the water dipoles are on average oriented by the negative ends to the cations at surface and thus

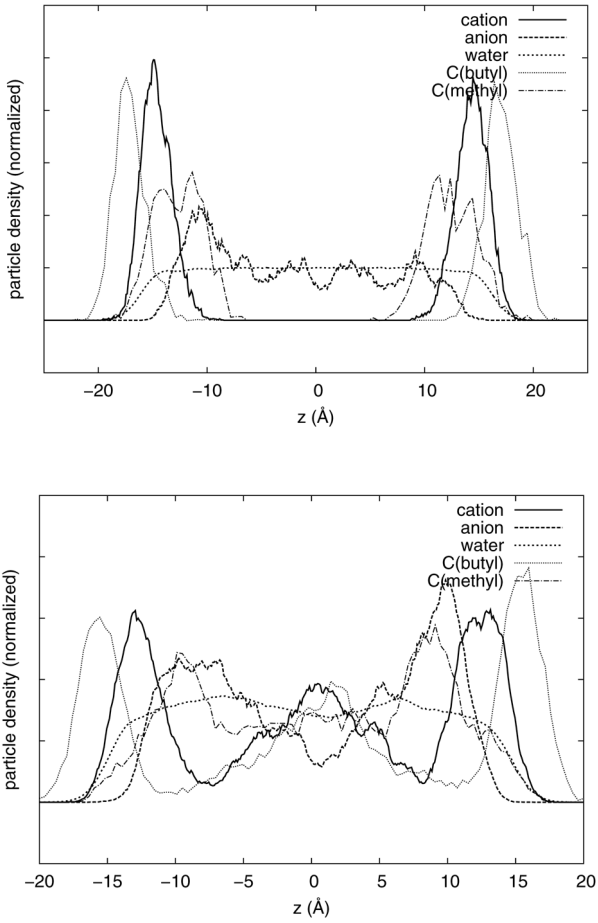

FIG. 2
Normalized density profiles of [BMIM]Cl in aqueous solution at 300 K. The total mole fraction is 0.0041 (top) and 0.0449 (bottom)

screen their charge. With growing concentration and thus with a saturation of the surface a second cation-rich layer in the middle of the slab can be observed. It is possible (with respect to the system size) that this is an indication of microaggregation of ions inside the liquid or even complete phase separation. This effect is more noticeable for [BMIM]Cl than for [OMIM]Cl, which has a longer alkyl chain and thus its solubility in water is lesser (and thus occupies the surface and its bulk concentration remains low).

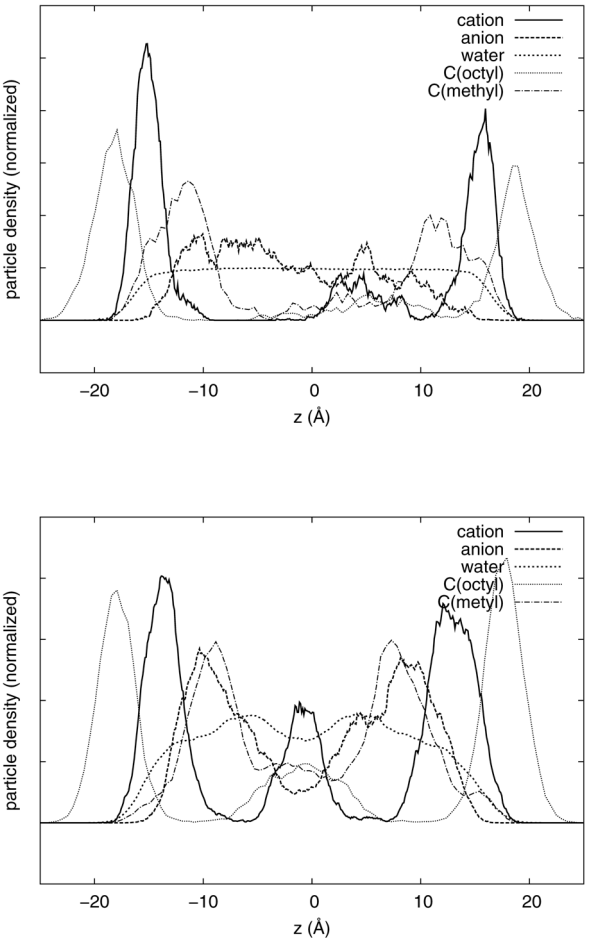

FIG. 3
Normalized density profiles of [OMIM]Cl in aqueous solution at 300 K. The total mole fraction is 0.0041 (top) and 0.0449 (bottom)

The surface has therefore a positive charge which can be verified by the charge density profiles in Figs 4 and 5.

Simulations of [BMIM]Cl at 300 K in a box of the same size but with 1500 molecules of water (thicker layer) were performed for comparison. Their outcomes are not presented here because the results are subject of a bigger uncertainty (low temperature and big system). From the density profiles it is evident that a new cation layer is really forming below the anion sublayer. This layer is populated less than the surface.

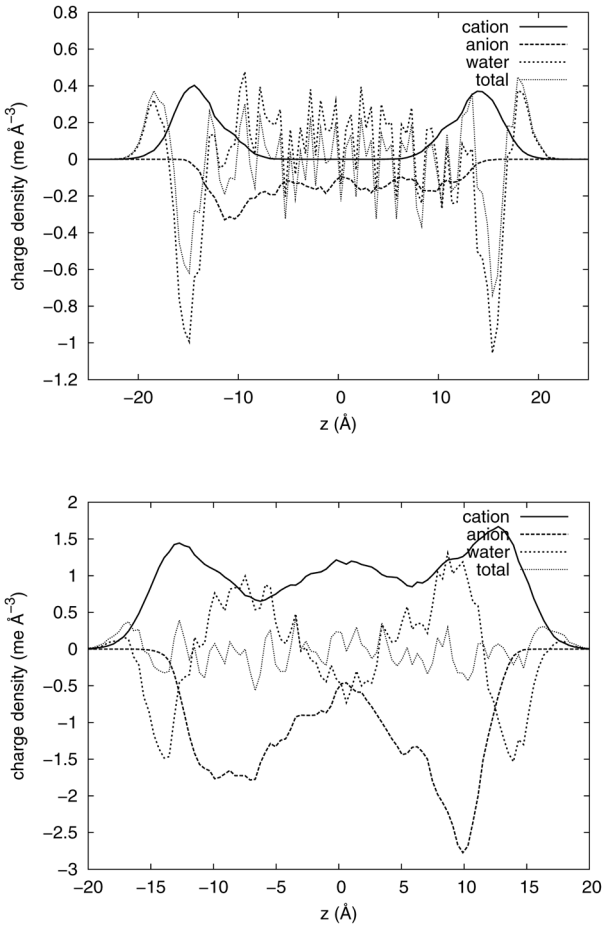

FIG. 4

Charge density profiles of [BMIM]Cl in aqueous solution at 300 K. The total mole fraction is 0.0041 (top) and 0.0449 (bottom)

From density profiles of individual groups it follows that the alkyl chains point preferably towards vacuum.

The orientation of the imidazolium ring at the surface can be described by angle β between the ring axis (vector perpendicular to the ring) and the surface normal (vector perpendicular to the surface). Because of symmetry, the second Legendre polynomial[25]

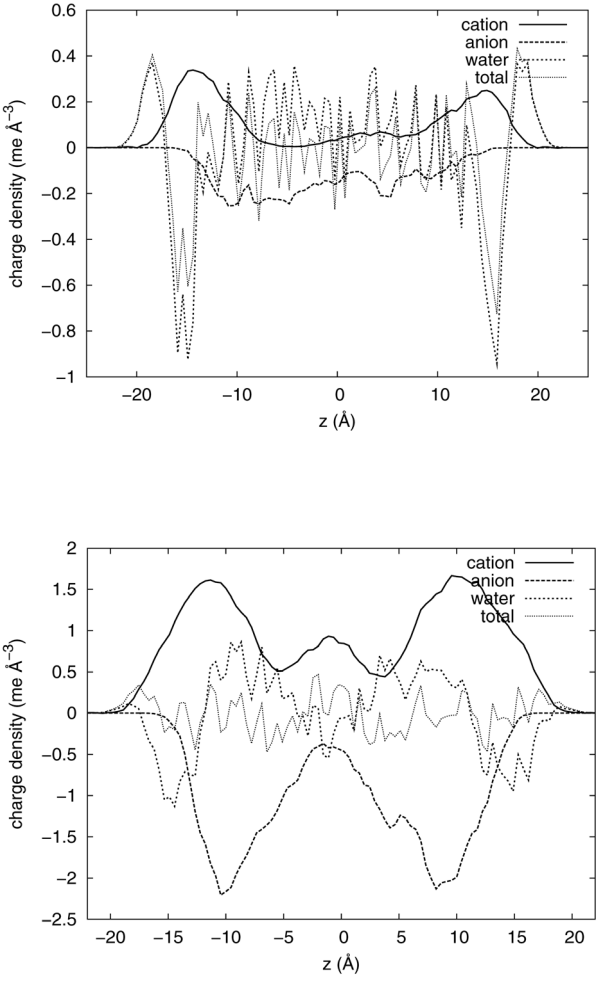

FIG. 5
Charge density profiles of [OMIM]Cl in aqueous solution at 300 K. The total mole fraction is 0.0041 (top) and 0.0449 (bottom)

$$P_2(\cos\beta) = (3\cos^2\beta - 1)/2 \qquad (2)$$

is needed to describe anisotropy in the ring orientations. We found that the averaged value of P_2 at the surface layer is positive, which means that the ring is preferentially parallel to the surface.

For a better insight into the system dynamics we also followed the trajectories (Fig. 6) of individual ions and counted "hopping" of ions between

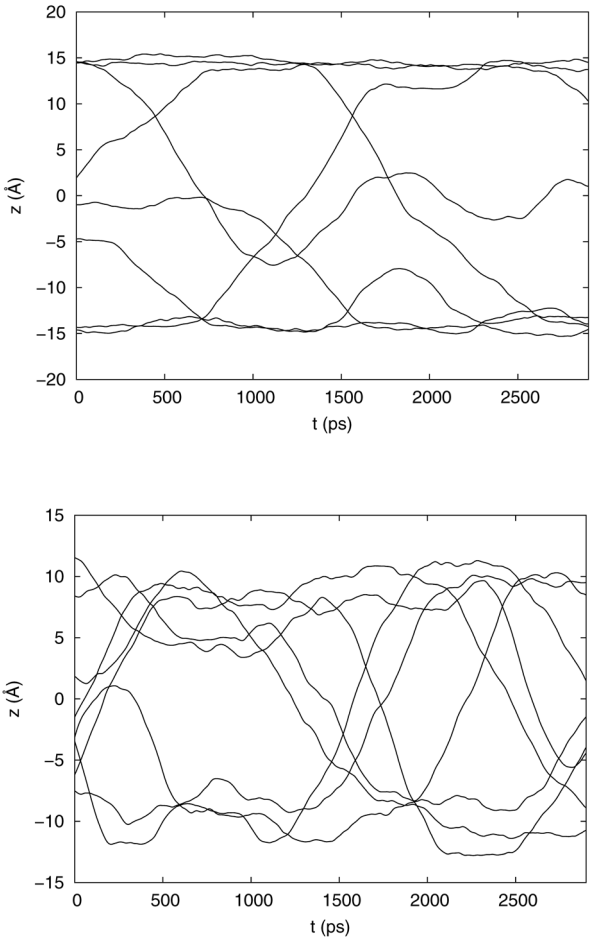

FIG. 6
A trajectory of cations (top) and anions (bottom) of [BMIM]Cl in the aqueous solution at 360 K. The system contained 8 ion pairs and 920 molecules of water

both surfaces, as in our previous work[16]. To define a "hopping event", we select a middle layer Δz = 10 Å thick; this is about 1/3 of the slab thickness. A hopping event occurs when a particle crosses this middle layer from one side to the other; e.g., it travels from the top third of the slab to the bottom third.

At low concentrations the cations are preferentially concentrated at the surface. In addition, the number of cation hopping events is very small and smaller than of anions which move freely in the bulk with only a small propensity towards surface. At the mole fraction of about 0.02 for $[BMIM]^+$ and 0.03 for $[OMIM]^+$, the number of the hopping events (per particle) of cations begins to increase. At about 0.05 the numbers of the hopping events of anions and cations are roughly equal and with further increasing mole fraction they decrease. This corresponds to the the region where the surface tension curve slows its sharp decrease and the surface gets saturated by cations. In other words, the motion of the cations is freest when the surface is fully saturated, but the cations yet do not aggregate in the bulk. With increasing concentration the number of hopping events per particle decreases while more and more anions come to the surface to compensate its positive charge.

From comparison with ref.[16], it is evident that the chloride anions move in the solution freer than $[BF_4]^-$ or $[PF_6]^-$ (about 2.5 flips/ion/ns for Cl^- at 360 K compared to roughly 1 for $[BF_4]^-$) (Fig. 7).

The hopping is sensitive to the diffusion in the *z*-direction, more precisely, to the slowest diffusion mode in this direction. The typical correlation time of this slowest mode is thus of the order of τ = 1 ns, i.e., comparable to the simulation length *t*. The asymmetry of the profiles is then proportional to $(t/\tau)^{-1/2}$. However, the "true" result is a symmetrized profile, which is not sensitive to odd diffusion modes. The first even mode of diffusion across the slab has the correlation time 4 times shorted, and the symmetrized profile is 2 times more accurate.

Surface Tension

The surface tension of both aqueous solutions of RTILs at both temperatures shows the expected trend (Fig. 8). The surface tension drops from that of pure TIP4P/2005 water to lower values. This corresponds to gradual saturation of the surface by ions.

Bowers et al.[9] measured the surface tension of aqueous solutions of $[BMIM][BF_4]$, [OMIM]Cl and [OMIM]I at 298 K. They found that the longer alkyl substituent at the imidazolium ring, the smaller is the concentration

of the minimum surface tension. For instance, the minimum occurs at an 8 times higher concentration for BMIM than OMIM.

Liu et al.[26] measured the physical properties of aqueous solutions of [BMIM][BF_4], [BMIM]Cl, [BMIM]Br and [EMIM]Cl at 298 K over a wide concentration range. They did not observe any minima for [BMIM]Cl.

An approximate comparison of simulated and experimental values is given in Table II. It is seen that the theoretical values are smaller, which can be atributed to the water model. The only exception is [OMIM]Cl at

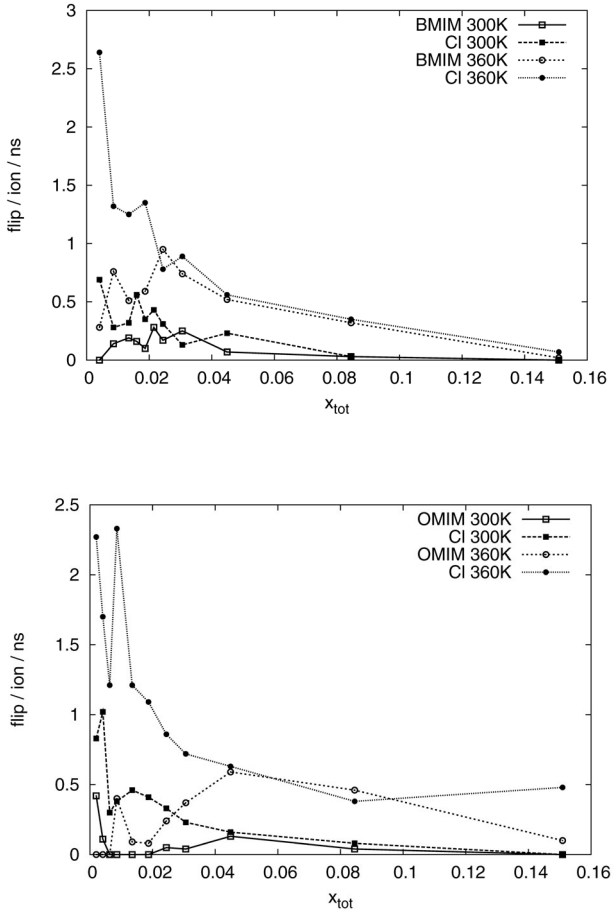

FIG. 7
Ion hopping between both surfaces in aqueous solutions as a function of total mole fraction. Top [BMIM]Cl, bottom [OMIM]Cl

1 mol/l. This disproportion may be caused by a bigger uncertainty in the simulated value and the increase of the surface tension after reaching the minimum[9].

We have not reproduced the experimentally observed minima, although we cannot exclude that at the lower temperature a small minimum might be hidden in the statistical noise. In all cases the surface tension decreases with concentration to the total mole fraction about 0.02–0.04 and then becomes constant or at least the decrease slows down. This "shoulder" ap-

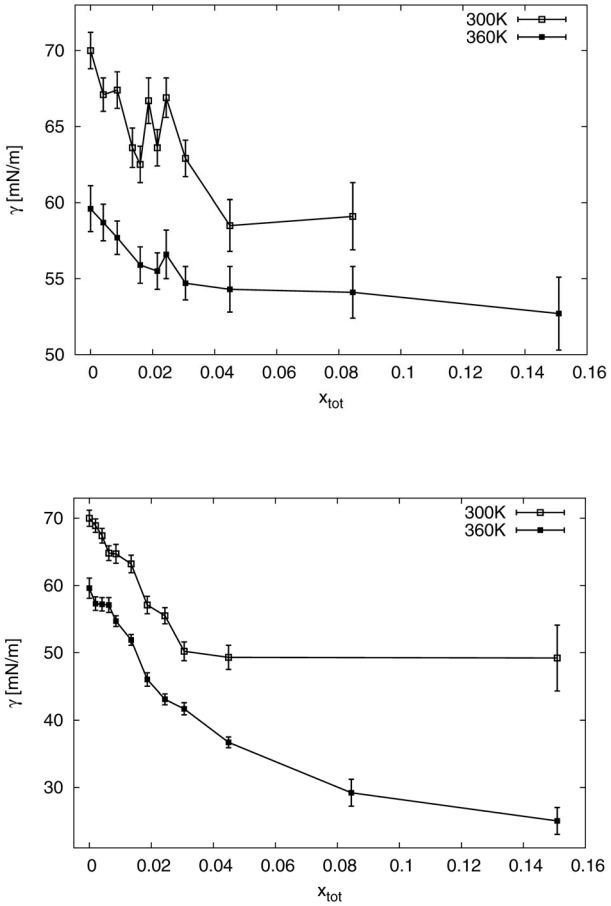

FIG. 8
Surface tension of aqueous solutions as a function of the total mole fraction. Top [BMIM]Cl, bottom [OMIM]Cl

TABLE II
A comparison of the simulated and experimental surface tension (in mN/m). Temperatures are 300 K for the simulated and 298 K for the experimental data. Concentration 0.01 mol/l was chosen as it corresponds to smallest simulated system, 1 mol/l was chosen as from this concentration the surface tension is nearly constant

Chlorides	c = 0.01 mol/l	c = 1 mol/l
[BMIM]Cl (exp. ref.[26])	71	65
[BMIM]Cl (this work)	67	60
[OMIM]Cl (exp. ref.[9])	70	43
[OMIM]Cl (this work)	69	49

pears at the total concentration where the surface becomes saturated. To be able to compare the shoulder position with the experimental position (of a shoulder and then a minimum), it is necessary to realize that the bulk concentration is lower than the total concentration. For [BMIM]Cl the bulk mole fraction is roughly one half of the total mole fraction and thus consistent with the experiment. The solubility of [OMIM]Cl is several times lower so is the bulk concentration, but it is difficult to make an accurate quantitative prediction; qualitatively the trend is correct (Note also that at the lowest concentration there is only one ion pair at each surface. Much larger system is necessary to achieve low concentrations with more ion pairs, which is costly.).

In both cases we may suggest, in agreement with ref.[16], that for reproducing of experimentally observed increase of surface tension it is necessary to employ polarizability. Moreover, for RTILs with long alkyl chain at the imidazole ring, larger systems are necessary.

CONCLUSIONS

We performed a series of molecular dynamics simulation of aqueous solutions of [BMIM]Cl and [OMIM]Cl.

The experimentally observed decrease of the surface tension was reproduced together with the populating of the surface by $[C_nMIM]^+$. The positive charge of the cationic layer is compensated by anions at higher concentrations and by water dipoles at lower concentrations. Alkyl chains are pointing towards vacuum, the imidazole rings lie preferably parallelly to the surface. The experimentally observed local minima and consecutive increase of the surface tension were not reproduced.

This work was supported by the Ministry of Education, Youth and Sports of the Czech Republic (Center for Biomolecules and Complex Molecular Systems, project LC512).

REFERENCES

1. Weingärtner H.: *Angew. Chem. Int. Ed.* **2008**, *47*, 654.
2. Adam D.: *Nature* **2000**, *407*, 938.
3. Hussey C. L.: *Pure Appl. Chem.* **1988**, *60*, 1763.
4. Seddon K. R.: *Kinet. Catal. (Transl. of Kinet. Katal.)* **1996**, *37*, 693.
5. Santos C. S., Rivera-Rubero S., Dibrov S., Baldelli S.: *J. Phys. Chem. C* **2007**, *111*, 7682.
6. Santos C. S., Baldelli S.: *J. Phys. Chem. C* **2008**, *112*, 11459.
7. Sung J., Jeon Y., Kim D., Iwahashi T., Iomori T., Seki K., Youchi Y.: *Chem. Phys. Lett.* **2005**, *406*, 495.
8. Sloutskin E., Ocko B. M., Tamam L., Kuzmenko I., Gog T., Deutsch M.: *J. Am. Chem. Soc.* **2005**, *127*, 7796.
9. Bowers J., Butts C. P., Martin P. J., Vergara-Gutierrez M. C.: *Langmuir* **2004**, *20*, 2191.
10. Law G., Watson P. R., Carmichael A. J., Seddon K. R., Seddon B.: *Phys. Chem. Chem. Phys.* **2001**, *3*, 2879.
11. Watson P. R., Law G.: *Chem. Phys. Lett.* **2001**, *1*, 345.
12. Gannon T. J., Law G., Watson P. R.: *Langmuir* **1999**, *15*, 8429.
13. Smith E. F., Rutten F. J. M., Villar-Garcia I. J., Briggs D., Licence P.: *Langmuir* **2006**, *22*, 9386.
14. Rivera-Rubero S., Baldelli S.: *J. Phys. Chem. B* **2006**, *110*, 15499.
15. Welton T., Cammarata L., Kazarian S. G., Salter P. A.: *Phys. Chem. Chem. Phys.* **2001**, *2*, 5192.
16. Picálek J., Minofar B., Kolafa J., Jungwirth P.: *Phys. Chem. Chem. Phys.* **2008**, *10*, 5765.
17. http//www.vscht.cz/fch/software/macsimus/index.html
18. Allen M. P., Tildesley D. J.: *Computer Simulations of Liquids*. Oxford University Press, Oxford 1987.
19. Liu Z., Huang S., Wang W.: *J. Phys. Chem. B* **2004**, *108*, 12978.
20. Abascal J. L. F., Vega C. J.: *Chem. Phys.* **2005**, *123*, 234505.
21. Frisch M. J., Trucks G. W., Schlegel H. B., Scuseria G. E., Robb M. A., Cheeseman J. R., Montgomery J. A., Vreven T., Kudin K. N., Burant J. C., Millam J. M., Iyengar S. S., Tomasi J., Barone V., Mennucci B., Cossi M., Scalmani G., Rega N., Petersson G. A., Nakatsuji H., Hada M., Ehara M., Toyota K., Fukuda R., Hasegawa J., Ishida M., Nakajima T., Honda Y., Kitao O., Nakai H., Klene M., Li X., Knox J. E., Hratchian H. P., Cross J. B., Bakken V., Adamo C., Jaramillo J., Gomperts R., Stratmann R. E., Yazyev O., Austin A. J., Cammi R., Pomelli C., Ochterski J. W., Ayala P. Y., Morokuma K., Voth G. A., Salvador P., Dannenberg J. J., Zakrzewski V. G., Dapprich S., Daniels A. D., Strain M. C., Farkas O., Malick D. K., Rabuck A. D., Raghavachari K., Foresman J. B., Ortiz J. V., Cui Q., Baboul Q. G., Clifford S., Cioslowski J., Stefanov B. B., Liu G., Liashenko A., Piskorz P., Komaromi I., Martin R. L., Fox D. J., Keith T., Al-Laham M. A., Peng C. Y., Nanayakkara A., Challacombe M., Gill P. M. W., Johnson B., Chen W., Wong M. W., Gonzalez C., Pople J. A.: *Gaussian 03*, Revision C.02. Gaussian, Inc., Wallingford (CT) 2004.

22. Berendsen H. J. C., Postma J. P. M., van Gunsteren W. F., DiNola A., Haak J. R.: *J. Chem. Phys.* **1984**, *81*, 3684.
23. Verlet L.: *Phys. Rev.* **1967**, *159*, 98.
24. Yeh I.-C., Berkowitz M. L.: *J. Chem. Phys.* **1999**, *111*, 3155.
25. Abramowitz M., Stegun I. A.: *Handbook of Mathematical Functions: With Formulas, Graphs and Mathematical Tables*, 9th ed., pp. 331–339 and 771–802. Dover Publications, New York 1972.
26. Liu W., Cheng L., Zhang Y., Wang H., Yu M.: *J. Mol. Liq.* **2008**, *140*, 68.